A COMBINED EXPERIMENTAL/NUMERICAL APPROACH TO STUDY THE THERMAL DISPERSION IN POROUS MEDIA FLOWS

by

Ehsan Mohseni LANGURI** and Krishna M. PILLAI

Laboratory for Flows and Transport Studies in Porous Media, University of Wisconsin, Milwaukee, Wis., USA

Original scientific paper
DOI: 10.2298/TSCI1110626009L

The non-isothermal transport during flow in porous media is studied for single- and dual-scale porous media. A new combined experimental/numerical approach to estimating the thermal dispersion tensor is introduced and applied for both isotropic (single-scale) and anisotropic (dual-scale) porous media. The equivalence between the heat and mass transfer is exploited and a 1-D flow experimental set-up is employed to study the spreading of a dye. Later, the mathematical model for such a spreading of concentration (equivalent to the temperature) around a point input in a constant velocity field is solved using the finite element based code COMSOL. Thus obtained numerical spreading pattern is fitted onto the experimentally observed one using the dispersion matrix (tensor) as a fitting parameter. A few cases of single- and dual-scale porous media are studied and the dispersion tensors are reported for each individual case. In one case, the results are validated with the available experimental data in the literature which shows a good match.

Key words: *porous media, thermal dispersion, fluid mechanics, heat transfer, dual-scale, single-scale*

Introduction

In this paper, our aim is to focus on the thermal dispersion term arising in the governing equation for non-isothermal flow through porous media. The thermal dispersion term exists as a result of both the micro-structure of the porous material as well as the heat convection effect. One of the most important applications of including thermal dispersion effect in the mathematical modeling of the heat equation is the manufacturing processes of polymer composites such as liquid composite molding [1]. In such technologies, the composites are created by impregnation of a preform with resin injected into the mold's inlet. This shows the importance of heat transfer and curing governing equations in the non-isothermal flow in both single-scale and dual-scale porous media.

Pillai and Munagavalasa [2] used a volume averaging method with the local thermal equilibrium assumption to derive a set of energy and species equations for dual-scale porous medium. The schematic view of the initial impregnation of such a medium by a liquid is presented in fig. 1(a). Unlike the single-scale porous media, there is an unsaturated region behind the moving flow-front in dual-scale porous media. The reason for such partial saturation can be mentioned as the flow resistance difference between the gap and the tows where the flow goes faster in the gaps rather than the wicking into the tows.

* Corresponding author; e-mail: ehsan@uwm.edu

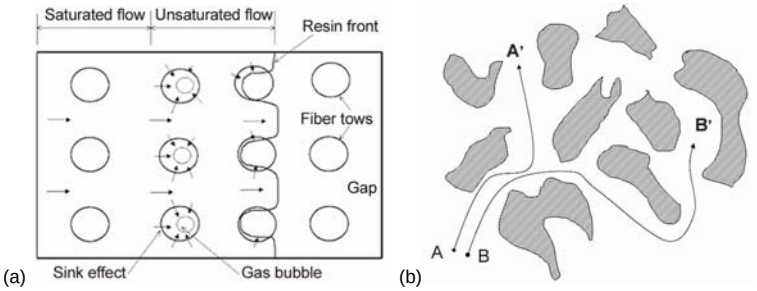

Figure 1. (a) Schematic view of the initial impregnation of a dual-scale porous-medium by a liquid [2], (b) mixing as a result of obstruction

Phelan *et al*. [3] showed that the conventional volume averaging method can be directly used to derive the transport equation for thermo-chemical phenomena inside the tows for single-scale porous media.

In some cases, a further complication arises in the thermal governing equation due to the presence of thermal dispersion [4] which happens due to the spreading of heat at the pore scale. Such spreading is mainly due to the molecular diffusion of heat as well as due to the hydrodynamic mixing caused by the random motion of fluid in a porous medium. Greenkorn [5] mentioned the following nine mechanisms for most of the thermal spreading at pore scale: (1) molecular diffusion: important in the case of sufficiently long time scales, (2) mixing due to obstructions: the flow channels in porous medium are tortuous means that fluid elements starting a given distance from each other and proceeding at the same velocity will not remain the same distance apart after a certain time, fig. 1(b), (3) existence of autocorrelation in flow paths: knowing all pores in the porous medium are not accessible to the fluid after it has entered a particular fluid path, (4) recirculation due to local regions of reduced pressure: the conversion of pressure energy into kinetic energy gives a local region of low pressure, (5) macroscopic or megascopic dispersion: due to non--idealities which change gross streamlines, (6) hydrodynamic dispersion: macroscopic dispersion is produced in capillary even in the absence of molecular diffusion because of the velocity profile produced by the adhering of the fluid wall, (7) eddies: turbulent flow in the individual flow channels cause the mixing as a result of eddy migration, (8) dead-end pores: dean-end pore volumes cause mixing in unsteady flow. The main reason is that as the solute rich front passes the pore, diffusion into the pore occurs due to molecular diffusion. After the front passes, the solute will diffuse back out and thus, disperse, (9) adsorption: it is an unsteady-state phenomenon where a concentration front will deposit or remove material and therefore tends to flatten concentration profiles.

Rubin [6] generalized the thermal governing equation as:

$$(\rho c)_m \frac{\partial T}{\partial t} + (\rho c)_f v \nabla T = \nabla(\mathbf{k}_m \nabla T) + q'''_m \tag{1}$$

where $\mathbf{k}_m$ is a second-order tensor called the dispersion tensor. Two dispersion phenomena that have been extensively studied in as part of the transport phenomena in porous media are the mass and thermal dispersions. The former involves the mass of a solute transported in a porous medium, while the latter involves the thermal energy transported in the porous medium. Due to the similarity of mass and thermal dispersions, they can be described using common dimensionless transport equation as:

$$\frac{\partial \langle \Omega \rangle}{\partial \theta} + \langle U_i \rangle \frac{\partial \langle \Omega \rangle}{\partial X_i} = \frac{1}{\mathrm{Pe}} \frac{\partial}{\partial X_i} \left(\mathbf{D}_{ij} \frac{\partial \langle \Omega \rangle}{\partial X_j} \right) \tag{2}$$

where $\langle \Omega \rangle$ is either the volume averaged concentration for mass dispersion, or the volume averaged dimensionless temperature for thermal dispersion, θ – the dimensionless time, $\langle U_i \rangle$ – averaged velocity vector, Pe – the Peclet number, and $\mathbf{D}_{ij}$ – the dispersion tensor of 2nd order. It should be noted that Pe = $uL/\mathcal{D}$ for mass dispersion, and Pe = uL/α for thermal dispersion where u and L are characteristic velocity and length, respectively. $\mathcal{D}$ and α are molecular mass and thermal diffusivities, respectively.

Most studies on the dispersion tensor so far have been focused on the *isotropic* porous media. Nikolaveskii [7] obtained the form of dispersion tensor for isotropic porous media by analogy to the statistical theory of turbulence. Bear [8] studied the relationship between the dispersive property of the porous media as defined by a constant of dispersion, the displacement due to a uniform field of flow, and the resulting distribution. He used a point injection subjected to a sequence of movements. The volume averaged concentration of the injected tracer, $\mathbf{C}_0$, around a point which is displaced at distance $L = ut$ in the direction of the uniform, isotropic, two dimensional field of flow from its original position is considered in his research:

$$\mathbf{C}(x, y; x_0, y_0) = \frac{C_0}{2\pi\sigma_x^{\,2}\sigma_y^{\,2}} \exp\left(-\frac{m^2}{2\sigma_x^{\,2}} - \frac{n^2}{2\sigma_y^{\,2}}\right) \tag{3}$$

where L is the distance of mean displacement, u – the uniform velocity of flow, t – the time of flow, σ_x and σ_y are standard deviations of the distribution in the x- and y-directions, respectively, and, finally m and n are the co-ordinates of the point (x, y) in the co-ordinate system centered at (ξ, η) given by $m = x - (x_0 + L)$ and $n = y - y_0$. Standard deviations are defined by $\sigma_x = (2D_I L)^{0.5}$ and $\sigma_y = (2D_{II} L)^{0.5}$ where D_I and D_{II} are the longitudinal and transverse constants of dispersion in porous media, respectively. One should note that the D_I and D_{II} used in the Bear work depend only upon properties of the porous medium such as porosity, grain size, uniformity, and shape of grains. From eq. (3), it follows that, after a uniform flow period, lines of the similar concentration resulting from the circular point injection of the tracer take the ellipse shape centered at the displaces mean point and oriented with their major axes in the direction of the flow:

$$\frac{x^2}{\sigma_x^{\,2}} + \frac{y^2}{\sigma_y^{\,2}} = 1 \tag{4}$$

Bear conjectured that the property which is defined by the constant of dispersion, D_{ijkl}, depends only upon the characteristics of porous medium and the geometry of its pore--channel system. In a general case, this is a fourth rank tensor which contains 81 components. These characteristics are expressed by the longitudinal and lateral constants of dispersion of the porous media. Scheidegger [9] used the dispersion tensor $\mathbf{D}_{ij}$ in the following form:

$$\mathbf{D}_{ij} = \mathbf{a}_{ijkm} \frac{v_k v_m}{|v|} \tag{5}$$

where v is the average velocity vector, v_k – the k^{th} component of velocity vector, $\mathbf{a}_{ijkm}$ – the fourth rank tensor called geometrical dispersivity tensor of the porous medium. Bear demonstrated how the dispersion tensor relates to the two constants for an isotropic medium: $a_{\parallel}$ is the longitudinal dispersion (along the mean flow direction), and $a_{\perp}$ – the transversal dispersion (perpendicular to the mean flow velocity).

For isotropic medium, the dispersion tensor can be expressed by longitudinal and transverse dispersion coefficients. If we consider the mean flow is along x-axis, $\mathbf{D}_{ij}$ can be written as:

$$\mathbf{D} = \begin{bmatrix} a_{\parallel} & 0 & 0 \\ 0 & a_{\perp} & 0 \\ 0 & 0 & a_{\perp} \end{bmatrix} \tag{6}$$

Therefore, transport equation can be written as:

$$\frac{\partial \langle \Omega \rangle}{\partial \theta} + \langle U_1 \rangle \frac{\partial \langle \Omega \rangle}{\partial X_1} = \frac{1}{\mathrm{Pe}} \left(a_{\parallel} \frac{\partial^2 \langle \Omega \rangle}{\partial X_1^2} + a_{\perp} \frac{\partial^2 \langle \Omega \rangle}{\partial X_2^2} + a_{\perp} \frac{\partial^2 \langle \Omega \rangle}{\partial X_3^2} \right) \tag{7}$$

It has been shown that one of the principle axes of the dispersion tensor in isotropic porous medium is along the mean flow direction. Unlike the isotropic media, there are nine independent components in the dispersion tensor for the case of *anisotropic* porous media. Bear [8] noted that the dispersion problem in a non-isotropic material still remains unsolved. He suggested to distinguishing between various kinds of anisotropies and doing statistical analysis with different frequency functions for the spatial distribution of channels in each case. Unless some specific types of porous media, such as the axisymmetric or transversely isotropic porous media are considered, it is not possible to simplify the form of dispersion tensor. In 1965, Poreh [10] used the theory of invariants to develop a dispersion tensor for the axisymmetric porous media. The average properties of an axisymmetric porous medium which affect the macroscopic dispersion pattern are invariants to rotation about given line. He established the general form of $\mathbf{D}_{ij}$ with two arbitrary vectors $\vec{\mathrm{R}}$ and $\vec{\mathrm{S}}$ as:

$$\mathbf{D}_{ij}\vec{\mathrm{R}}_i\vec{\mathrm{S}}_j = B_1\delta_{ij}\vec{\mathrm{R}}_i\vec{\mathrm{S}}_j + B_2 v_i v_j \vec{\mathrm{R}}_i\vec{\mathrm{S}}_j + B_3\lambda_i\lambda_j\vec{\mathrm{R}}_i\vec{\mathrm{S}}_j + B_4 v_i\vec{\mathrm{R}}_i\lambda_j\vec{\mathrm{S}}_j + B_5\lambda_i\vec{\mathrm{R}}_i v_j\vec{\mathrm{S}}_j \tag{8}$$

where λ is the axis of symmetry, B_1, B_2, B_3, B_4, and B_5 are arbitrary functions of v^2 and $v_k\lambda_k$. For arbitrary $\vec{\mathrm{B}}$ and $\vec{\mathrm{S}}$ and symmetric $\mathbf{D}_{ij}$, one can have:

$$\mathbf{D}_{ij} = B_1\delta_{ij} + B_2 v_i v_j + B_3\lambda_i\lambda_j + B_4(v_i\lambda_j + \lambda_i v_j) \tag{9}$$

The dimensionless form of eq. (7) is obtained as:

$$\frac{\mathbf{D}_{ij}}{D_0} = G_1\delta_{ij} + G_2\left(\frac{l^2}{D_0^2}\right)v_i v_j + G_3\lambda_i\lambda_j + G_4\left(\frac{l}{D_0}\right)(v_i\lambda_j + \lambda_i v_j) \tag{10}$$

where G_1, G_2, G_3, and G_4 are dimensionless functions of $(vl/D_0)^2$, $(vl/\upsilon)^2$. D_0 is the molecular diffusivity coefficient, l – the length characterizing the size of pores, and υ – the kinematic viscosity. The final form of the dispersion tensor for axisymmetric porous media can be given as:

$$\frac{\mathbf{D}_{ij}}{D_0} = \left(\beta_1 + \beta_2\frac{v^2l^2}{D_0^2}\right)\delta_{ij} + \beta_3\left(\frac{l^2}{D_0^2}\right)v_i v_j + \left(\beta_4 + \beta_5\frac{v^2l^2}{D_0^2}\right)\lambda_i\lambda_j + \beta_6\left(\frac{vl^2}{D_0^2}\right)(v_i\lambda_j + \lambda_i v_j) \tag{11}$$

where β_1 and β_4 are dimensionless numbers, β_2, β_3, and β_5 are even functions of $\cos\omega$, and β_6 is an odd function of $\cos\omega$.

By assuming no motion within an axisymmetric medium, $\mathbf{D}_{ij}$ is simplified to:

$$\frac{\mathbf{D}_{ij}}{D_0} = \beta_1 \delta_{ij} + \beta_4 \lambda_i \lambda_j \tag{12}$$

Equation (12) indicating that one of the principal axes of $\mathbf{D}_{ij}$ is, in this case, co-directional with λ. Bear [8] also noted that his analysis was based on an unproved assumption that $\mathbf{D}_{ij}$ may be expanded in a power series.

In 1967, Whitaker [11] applied point-wise volume-averaging method for transport equation in anisotropic porous media and obtained the dispersion tensor $\mathbf{D}_{ij}$ as:

$$\mathbf{D}_{ij} = D_0(\delta_{ij} + R\vec{\mathrm{B}}_{ij}) + C_{ikj} v_k + E_{ikmj} v_k v_m \tag{13}$$

where the second order tensor $\vec{\mathrm{B}}_{ij}$ is a function of tortuosity vector:

$$\tau_j = \int_S \Omega n_j \mathrm{d}s \tag{14}$$

The third-order tensor $\mathbf{C}_{ikj}$ is given by:

$$\mathbf{C}_{ikj} = \frac{\partial^2 \left\langle \tilde{\Omega} \tilde{v}_i \right\rangle}{\partial \left\langle v_k \right\rangle \partial \left(\dfrac{\partial \left\langle \Omega \right\rangle}{\partial x_j} \right)} \tag{15}$$

The fourth-order tensor $\mathbf{E}_{ikmj}$ is introduced as:

$$\mathbf{E}_{ikmj} = \frac{\partial^3 \left\langle \tilde{\Omega} \tilde{v}_i \right\rangle}{\partial \left\langle v_k \right\rangle \partial \left\langle v_m \right\rangle \partial \left(\dfrac{\partial \left\langle \Omega \right\rangle}{\partial x_j} \right)} \tag{16}$$

where $\tilde{\Omega}$ is the deviation of concentration or temperature from the average, and $\tilde{v}_i$ – the velocity deviation:

$$\tilde{\Omega} = \Omega - \left\langle \Omega \right\rangle^f \quad \text{and} \quad \tilde{v}_i = v_i - \left\langle v_i \right\rangle^f \tag{17}$$

One should keep in mind that from eqs. (15) and (16), we know that $\mathbf{C}_{ikj}$ and $\mathbf{E}_{ikmj}$ are completely symmetrical. Patel and Greenkorn [12] suggested that Whitaker's expression for dispersion tensor is the correct one for anisotropic media.

A combined experimental/numerical approach is introduced for the estimation of the dispersion tensor in the heat-transfer governing equation of non-isothermal flow through porous media. The experimental set-up and the finite element method procedure will be defined in the following sections. Using the experiment data in numerical simulation leads to an accurate estimation of dispersion tensor in the single-scale and dual-scale porous media. This is first such attempt to explore thermal dispersion term through a combined experimental/numerical method, especially in dual-scale porous media characterized by a complex micro-structure [13].

Proposed experimental/numerical method

A new combined experimental/numerical method for predicting the dispersion tensor is introduced and applied in this paper. Using this method, one can estimate the thermal dispersion tensor for different types of fiber mats characterized as isotropic and anisotropic porous media. In this method, a numerical modeling comes along with an experimental set-up where the combination of both results leads to prediction of the dispersion tensor. Since mass and thermal dispersions are very similar in the transport mechanism in porous media, they can be described using the dimensionless transport equations, eq. (2). We are employing the analogy between the concentration governing equation (in our experimental set-up) and the temperature governing equation (in our numerical modeling) to identifying the dispersion tensor. In this prediction, the growth of the initially circular tracer (dye) with time is studied. The results of the dye expansion at different timeframes are compared with results from our numerical model. Once the numerical model's result is adjusted the same as the one from experiments at a specific time, the dispersion tensor is obtained from the corresponding tensor components used in the numerical simulation. Therefore, the dispersion tensor in the numerical modeling is the filling parameter used in order to match the numerical results with the results obtained from the experiments.

Experimental set-up

The experimental section of this combined experimental/numerical method is done using the 1-D flow experiment set-up. In order to run the set-up, a stack of fiber-glass mat (called preform) is placed inside the mold cavity, fig. 2(a). Two sides of the preform in the horizontal plane are sealed using the removable glue in order to avoid the leaking and race tracking along the sides during the experiment. The mold is then closed and sealed tightly. The top layer of the mold is made out of a Polycarbonate material which is clear and allows observation of the flow behavior in the porous media. The test fluid is injected from one end of the mold and an outlet is designed at another end of the mold. A pressure transducer is connected at the top of the mold to record the inlet pressure history, fig. 2(b).

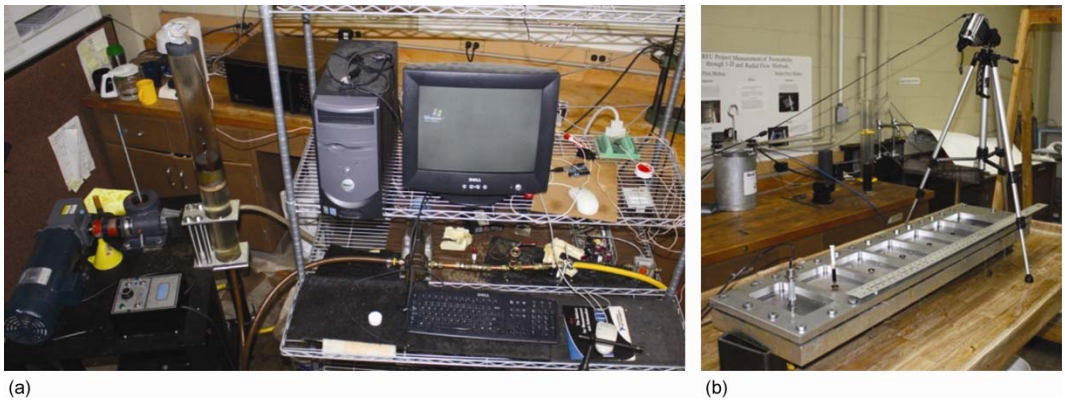

Figure 2. The 1-D flow experiment set-up, (a) data acquisition system, (b) the 1-D mold set-up
(for color image see journal web-site)

A video camera is located on the top of the mold with the clear top mold to record the flow process during the experiments. The camera equipped with a digital timer and a measuring bar located along the mold length and facing to the camera are employed to estimate

the velocity of tracer liquid at different times. A syringe filled with the dye (methylene blue) is placed at the flow inlet to inject the colored dye into the steady flow of liquid through the fiber mats.

The test fluid injection system is designed to inject the liquid at a constant volume flow-rate that can be monitored through a computer. The flow injection system consists of a steel cylinder floating in a larger polycarbonate cylinder filled with the test liquid. The floating cylinder is connected to a level gage for monitoring the level of test liquid inside the large cylinder. A feedback system using the level gage is employed on this flow-meter set-up in order to keep the injection at a steady level for a constant flow-rate experiment. The test liquid is composed of 50% corn syrup and 50% water. The corn syrup is white and hence, the blue dye injected at the inlet of the mold has a good color contrast with the test liquid. The density of the corn syrup and water mixture is measured by weighing a specific volume of liquid using a weighing balance. The dynamic viscosity of the test liquid is obtained by using a Brookfield viscometer and the porosity of the porous material inside the mold cavity is estimated by submerging the porous material inside a graduated cylinder filled with water. These physical measurements are conducted several times and averaged in order to have a reasonable property value.

Once the whole 1-D flow experiment set-up is ready, it can be run at different flow rates with different porosities as well as different porous media micro-structures corresponding to the single- and dual-scale porous media. The blue dye is injected when the test liquid is passing through the porous material under steady-state condition. The dispersion of injected dye is visible due to the contrast of its color with the test liquid's color. In order to complete this combined experimental and numerical method, the numerical results should accompany the experimental data so that the dispersion terms can be estimated.

Numerical method

The transient energy equation is solved by means of the finite element method using COMSOL multiphysics software. Fluid properties as well as the porous-material porosity are used as parameters to solve the transient energy equation. Boundary conditions and initial conditions are assumed for the created geometry, fig. 3.

The initial temperature (or initial concentration) distribution in the form of a circle is assumed inside the geometry, close to the inlet. The test fluid (corn syrup-water mixture) is injected from left inlet boundary which flows out from the right outlet boundary.

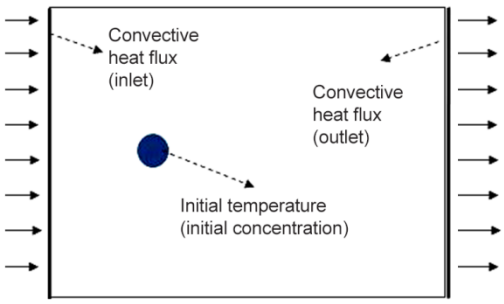

Figure 3. Schematic view of the geometry, the boundary and initial conditions

Results and discussions

The dispersion in porous media occurs due to the combined effects of molecular diffusion and convection of flow in pore spaces. In order to have a better understanding of the effect of molecular diffusion is studied individually. Figure 4 shows the effect of molecular diffusion on thermal dispersion in porous media where there is no convection during heat transfer. A 2×2 unit matrix is assumed as the dispersion coefficient for this case which leads to a full circular expansion due to similar diffusion in both horizontal and vertical directions.

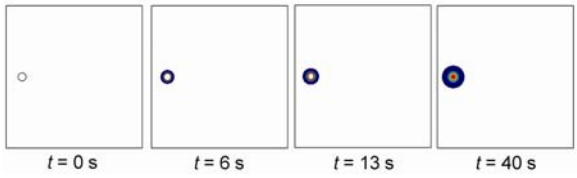

Figure 4. Effect of pure molecular diffusion of thermal dispersion by time (for color image see journal web-site)

To gain physical insights of the aforementioned method, the dispersion results of the experimental modeling and finite element method are compared. Constant flow-rate of Q = = 2 ml/s through the random fiber mat, a single-scale porous medium, fig. 5, with porosity of $\varepsilon = 0.8$ at three different time frames are considered here.

In order to estimate the dispersion tensor in such a single-scale porous medium, the experimental observation has to be matched with the numerical simulation results. Three different time frames are assumed for this analysis.

Figure 5. (a) Random fiber-glass mat as a representative of single-scale porous media, (b) stitched fiber-glass mat as a representative of dual-scale porous media, (c) unidirectional fiber-glass as a representative of dual-scale porous media (for color image see journal web-site)

The mentioned combined experimental/numerical method tries to estimate the dispersion tensor by matching the experimental data for longitudinal and transverse terms of dispersion by those in the numerical simulation. Results of the proposed experimental/numerical approach give the dispersion tensor of:

$$\mathbf{D} = \begin{bmatrix} 1.062E-7 & 0 \\ 0 & 3.186E-8 \end{bmatrix}$$

for the random porous media as a representative of a single-scale porous medium, fig. 6. For this single-scale porous medium, the flow direction along the mold horizontal direction and the corresponding vertical direction are the longitudinal and transverse directions, respectively, for the dispersion tensor. Our results for three different flow-rates (Q = 1 ml/s, Q = 2 ml/s, and Q = 3 ml/s) show that the dispersion tensor remains the same for this type of porous media.

For the sake of validation, a comparison has been done between our results and the results from an available model [14] as:

$$D_{\parallel} = \lim_{x \to \infty} \frac{U^3 \Delta t^2}{2x} \tag{18}$$

Equation (18) models the longitudinal dispersion coefficient of the injected tracer particles at the inlet of the porous medium sample. In this equation, U is the mean tracer velocity which covers distance x in Δt seconds. In order to validate our results with this model, two different time frames were selected and the velocity, Δt, and the distanced traveled are substituted in eq. (18).

The porous medium is assumed to be isotropic for this section. The tracer is moving with a speed u = 0.0002 m/s at the initial location of x = 0.070 m at t = 36 s to the next location of x = 0.090 m at t = 40 s. Following eq. (18), the longitudinal dispersion is $D = 3.20 \cdot 10^{-7}$ while the longitudinal dispersion predicted by our combined experimental/numerical method is $D = 3.19 \cdot 10^{-7}$. One can see that there is a good match between our results and those obtained from eq. (18) for the longitudinal dispersion in the random fiber mat.

A study on the changing dimensions of the expanding tracer-generated ellipse in the considered single-scale porous medium is presented in fig. 7. This picture shows the increase in the longitudinal and transverse dimensions of the initial circular dye-batch with time. One can notice a rapid expansion along the longitudinal direction compared to the transverse direction due to the present convection effects along the flow direction.

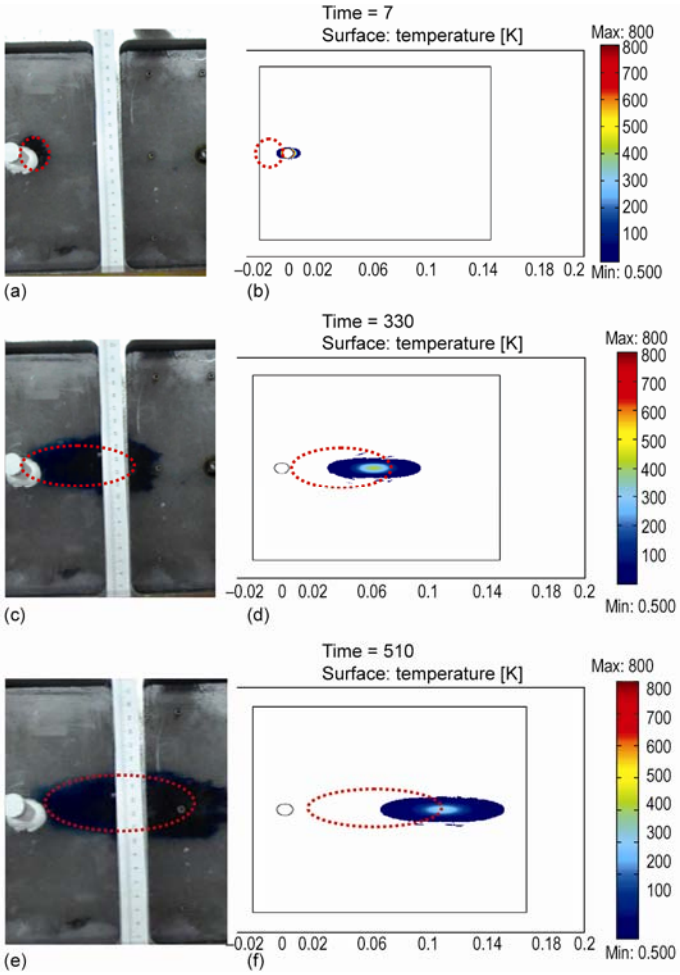

Figure 6. Matching the experimental and numerical results for a single-scale porous medium (random fiber mat) at Q = 2 ml/s at three different time frames of (a) 7 s, (b) 33 s, and (c) 51 s (for color image see journal web-site)

Similar study was carried out on a dual-scale porous medium for the purpose of estimation of the dispersion tensor, fig. 5(b). Experimental observations along with the numerical simulation results are matched in order to estimate the dispersion tensor.

An important characteristic of the stitched fiber-glass (as a type of dual-scale porous media used in the experiments) is its symmetry along the tows and the corresponding vertical direction. This anisotropic porous medium is assumed as a

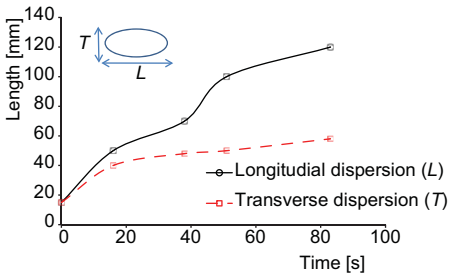

Figure 7. The longitudinal and transverse increases of the initial circular dye-patch with time

periodic porous medium in the two directions. Analysis on this type of porous media through the experiments and computer simulations are presented in fig. 8.

Based on the symmetry present in this anisotropic periodic porous medium, the dispersion of heat (or concentration) has to be symmetric with respect to the direction of the flow. The prediction for this case gives:

$$\mathbf{D} = \begin{bmatrix} 3.186E-7 & 0 \\ 0 & 1.062E-8 \end{bmatrix}$$

Another anisotropic porous medium studied in this chapter is the unidirectional glass-fiber mat shown in fig. 5(c). The dual-porosity effect in this unidirectional porous medium causes an unsaturated flow-front to appear during the mold-filling process. The microstructure of the unidirectional mat is such that the flow initially moves between tow bundles, fig. 9(a). Once the channel between the tow bundles is filled with the test fluid, it begins to wet the tow bundles from sides which slows the liquid front. However, one tows are saturated, the injected liquid flows in the gap region only, fig. 9(b).

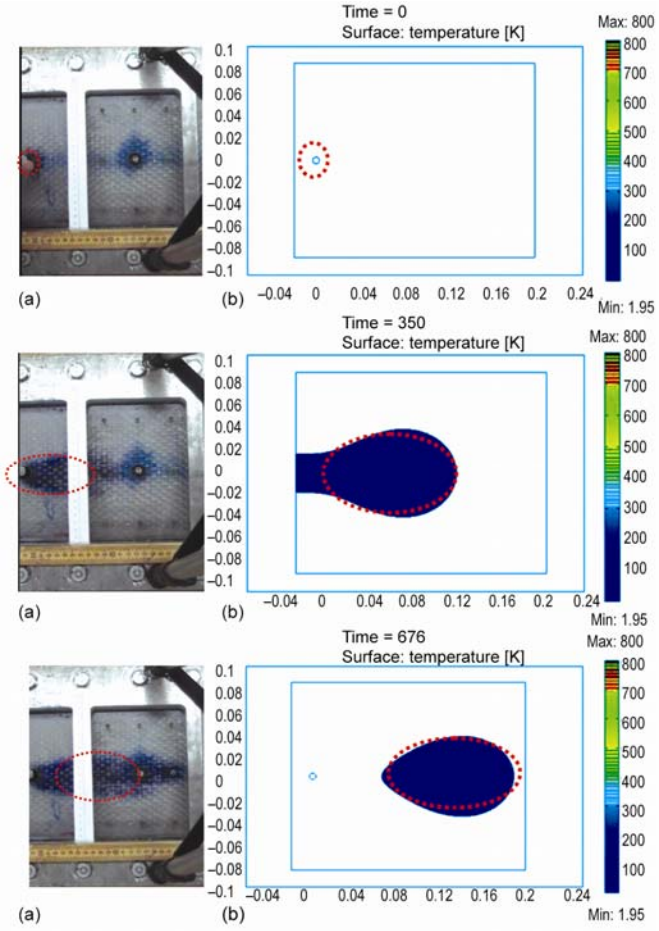

Figure 8. Comparison of the experimental and numerical modeling for an anisotropic but periodic medium at Q = 2 ml/s; (a) experimental results at t = 0 s, (b) numerical results at t = 0 s, (c) experimental results at t = 35 s, (d) numerical results at t = 35 s, (e) experimental results at t = 71 s, and (f) numerical results at t = 71 s
(for color image see journal web-site)

Based on these reasons, the actual flow-rate in channels under steady-state conditions is much more than the Darcy velocity.

$$u_{\text{channel}} = \frac{Q}{A_{cs,\text{channel}}} \gg \frac{Q}{A_{cs,\text{cavity}}} = u_{\text{Darcy}} \tag{19}$$

Results obtained from experiments confirm this theoretical prediction. The velocity of the dye inside the channels between the tow bundle (u_{channel} = 0.068 m/s) is an order of magnitude larger than theoretical Darcy velocity (u_{Darcy} = 0.0050 m/s). Figure 10 depicts the tracer movements through the unidirectional mat channels with a much higher velocity compared to the Darcy velocity.

According to these reasons, the dispersion tensor for this type of fiber glass is not estimated here. The Darcy's law is not obeyed in the entire domain. This type of problem should be handled separately by assuming two flows (*i. e.*, gap and tow region flows) with different velocities.

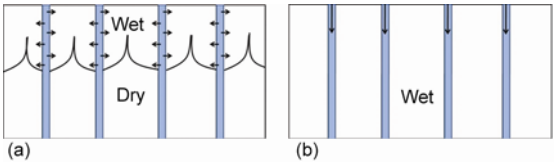

Figure 9. Unidirectional fiber-glass in (a) initial unsaturated flow, and (b) saturated flow

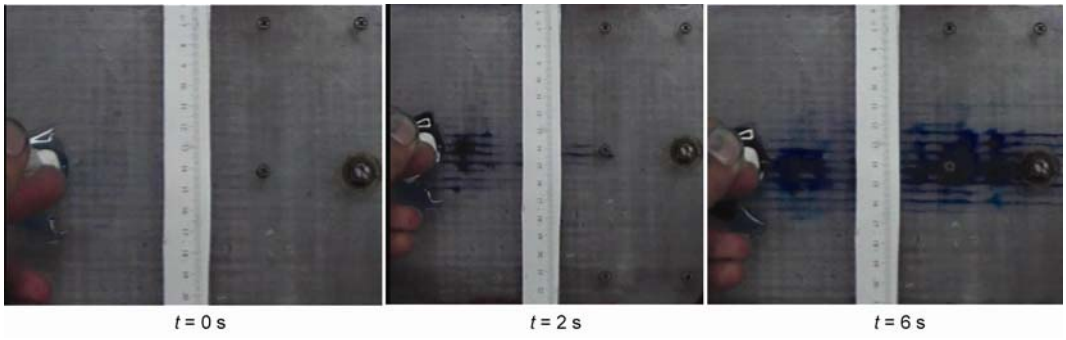

Figure 10. Experimental observation of flow of tracer through a dual-scale porous medium made of the unidirectional fiber mats (for color image see journal web-site)

Conclusions

In this paper, the non-isothermal flow through porous media is studied experimentally and numerically. An effort was made to quantify the thermal dispersion effect which enhances heat transfer in porous-media flows. A combined experimental/numerical approach to estimate the thermal dispersion during the non-isothermal flow in porous media is described. Both single-scale and dual-scale porous media were considered. Studies were done over three different mass flow-rates. The estimated longitudinal thermal dispersion value in single-scale porous media is compared with available results in the literature. The validation study showed a very good match, and hence, motivated us to explore this method for the dual-scale porous media. Preferential flow through channels frustrated our efforts to apply the proposed experimental/numerical approach to model thermal dispersion in the unidirectional stitched mat.

References

[1] Rudd, C. D., *et al*., *Liquid Molding Technologies,* Woodhead Publishing Ltd., Philadelphia, Penn., USA, 1997

[2] Pillai, K. M., Munagavalasa, M. S., Governing Equations for Unsaturated Flow through Woven Fiber Mats, Part 2, Non-Isothermal Reactive Flows, Composites, Part A, *Applied Science and Manufacturing, 35* (2004), 4, pp. 403-415

[3] Phelan, F. R., Jr., *Modeling of Microscale Flow in Fibrous Porous Media,* Springer-Verlag New York, USA, 1991

[4] Nield, D. A., Bejan, A., *Convection in Porous Media,* 3rd ed. Springer, New York, USA, 2006

[5] Greenkorn, R., A., *Flow Phenomena in Porous Media*, Marcel Dekker, Inc., New York, USA, and Basel, Switzerland, 1983

[6] Rubin, H., Heat Dispersion Effect on Thermal Convection in a Porous Medium Layer, *J. Hydrol., 21,* (1974), 2, pp. 173-184

[7] Nikolaevskii, V. N., Convective Diffusion in Porous Media, *Journal of Applied Mathematics and Mechanics, 23* (1959), 6, pp. 1492-1503
[8] Bear, J., On the Tensor Form of Dispersion in Porous Media, *Journal of Geophysical Research*, *66* (1961), 4, pp. 1185-1197
[9] Scheidegger, A. E., General Theory of Dispersion in Porous Media, *Journal of Geophysical Research, 66* (1961), 10, pp. 3273-3278
[10] Poreh, M., The Dispersivity Tensor in Isotropic and Axisymmetric Mediums, *Journal of Geophysical Research* (1965), 70, pp. 3909-3913
[11] Whitaker, S., Diffusion and Dispersion in Porous Media, *AIChE Journal, 13* (1967), 3, pp. 420-427
[12] Patel, R. D., Greenkorn, R. A., On Dispersion in Laminar Flow through Porous Media, *AIChE Journal, 16* (1970), 2, pp. 332-334
[13] Languri, E. M., Isothermal and Non-Isothermal Flows in Porous Media, Ph. D. thesis, University of Wisconsin, Milwaukee, Wis., USA, 2011
[14] Bouchaus, J. P., *et al.*, Anomalous Diffusion in Disordered Media: Statistical Mechanisms, Models and Physical Applications, *Phys. Rep. 195* (1990), pp. 127-293

Paper submitted: June 26, 2012
Paper revised: January 14, 2013
Paper accepted: January 14, 2013